

Some recent results on global modeling of oceanic mesoscale eddies, barotropic tides, and baroclinic tides

Brian K. Arbic

Department of Oceanography
and
Center for Ocean-Atmospheric Prediction Studies (COAPS)
Florida State University

Spring 2009

Supported by funding from NSF, NRL, and ONR

Introduction

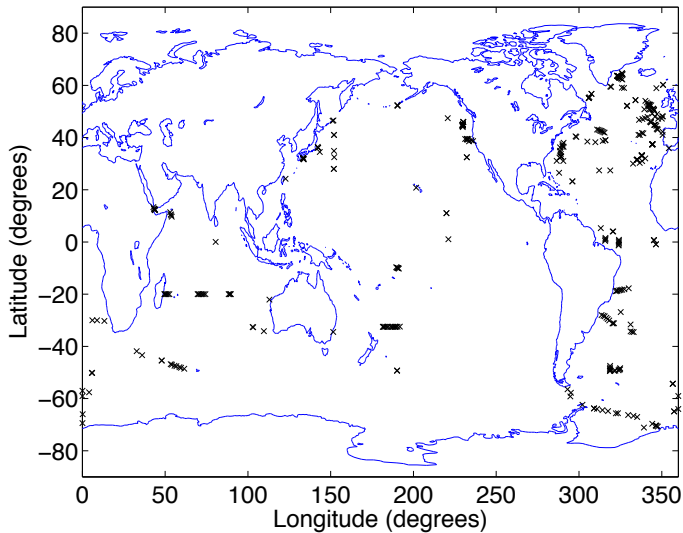
Will present brief overviews of three lines of research into the dynamics and energy budgets of tides and the eddying general circulation. All three lines utilize global models.

- Estimates of bottom flows and bottom boundary layer dissipation of the oceanic general circulation from global high-resolution models (Arbic, Shriver, Hogan, Hurlburt, McClean, Metzger, Scott, Sen, Smedstad, and Wallcraft, *Journal of Geophysical Research* 2009)
- Resonance of barotropic tides, with particular focus on "back-effect" of shelves upon open-ocean tides (Arbic, Karsten, and Garrett, under review for special issue of *Atmosphere-Ocean*, Arbic and Garrett, under review for special issue of *Continental Shelf Research*)
- Concurrent simulation of tides and the general circulation in an eddy-resolving global ocean model (Arbic, Wallcraft, and Metzger, to be submitted shortly)

Motivation–Part I (BBL dissipation of general circulation)

- With some exceptions (e.g. Penduff et al. 2006), extensive comparisons of realistic high-resolution models with subsurface data are rare—here we compare bottom flows in models to those in current meters.
- Horizontal length scales, vertical structure, and amplitude of eddy kinetic energy in idealized geostrophic turbulence models compare most closely to observations when bottom drag is moderately strong (Arbic and Flierl 2004, Arbic et al. 2007, Arbic and Scott 2008).
- Suggests BBL drag may be important for dynamics and energy budget of general circulation, which is fed by ~ 1 TW of wind energy (e.g. Wunsch 1998).

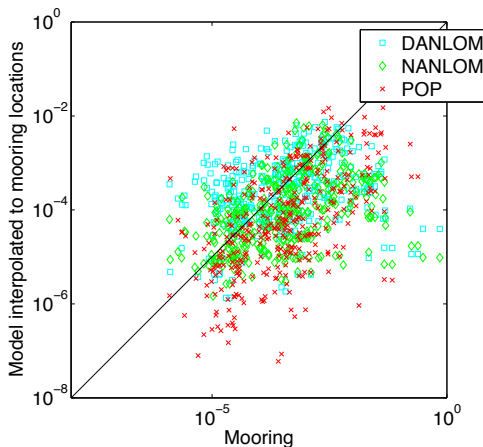
Location of moored near-bottom current meters



Models used

- DANLOM: Data-assimilative NLOM (4384×8192 gridpoints; 6 Lagrangian layers)
- NANLOM: Non-assimilative NLOM (4384×8192 gridpoints; 6 Lagrangian layers)
- POP: 2400×3600 gridpoints, 40 z-levels

Scatterplots—models vs moored current meters



Both axes show $\overline{|\mathbf{u}_{bottom}|^3}$ in units of $m^3 s^{-3}$

Averages over abyssal mooring sites of bottom flows—models vs current meters

$$\gamma = \frac{\sum_{i=1}^{274} |\mathbf{u}_{\text{bottommodel},i}|^3}{\sum_{i=1}^{274} |\mathbf{u}_{\text{bottommooring},i}|^3}$$

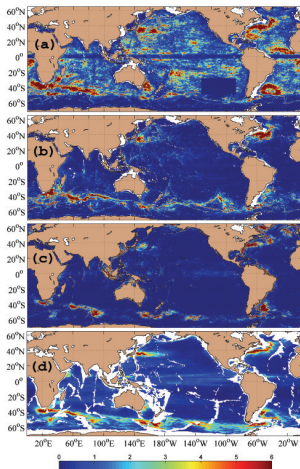
- Computed over 274 abyssal current meters

Model	γ
DANLOM	0.73
NANLOM	0.37
POP	0.40

- Paper includes much more detail:
 - comparison in North Atlantic with North Atlantic POP model also included
 - comparison as function of seafloor depth
 - comparison using other measures of model than interpolated values shown here

Maps (mW m^{-2}) and global integrals (TW) of time-averaged dissipation

(a) DANLOM, (b) NANLOM,
(c) POP, (d) Sen et al. (2008)



$$\bullet [\overline{D}] = \int \rho c_d \overline{|\mathbf{u}_b|^3} dA$$

• Native

$c_d = 0.003/0.002/0.001225$ for
DANLOM/NANLOM/POP

• Common $c_d = 0.0025$ (used
in maps to left)

Model	c_d	$[\overline{D}]$
DANLOM	Native	0.65
NANLOM	Native	0.16
POP	Native	0.14
DANLOM	Common	0.54
NANLOM	Common	0.20
POP	Common	0.29

Summary–Part I (BBL dissipation of general circulation)

- Bottom flows in NLOM and POP do not compare well to those in current meters on a point-by-point basis, but compare well in an average sense, suggesting they may provide reasonable estimates of globally integrated dissipation by bottom boundary layer drag.
- Globally integrated dissipations range from 0.14 to 0.65 TW, a substantial fraction of wind-power input. Since range of estimates is wide, other dissipation mechanisms cannot be ruled out.
[Nikurashin 2008–breaking of internal waves generated by currents and eddies over rough topography. Müller et al. 2005–energy transfer to submesoscale fronts. Polzin 2008–energy transfer to internal waves.]
- Follow-up work includes Rob Scott and high school student Anson Varghese taking lead on comparison of many high-resolution models to current meters throughout the entire water column, not just at bottom.

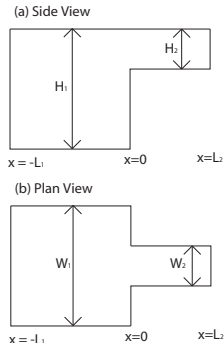
Central questions–Part II (Resonance of barotropic tides)

- What are the factors that control the resonance of tides in the open and coastal oceans?
- Is there a “back-effect” of the shelf tides upon the open-ocean tide?
- How do tides respond to changes in sea level, for instance to the ~130 m lower sea levels of the ice ages?

Motivated in part by...

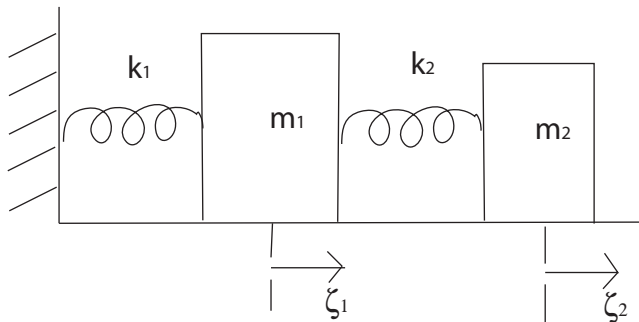
- Studies of coastal resonances e.g. Garrett 1972, Arbic, St-Laurent, Sutherland, Garrett 2007, Cummins, Karsten, Arbic, in review for special issue of *Atmosphere-Ocean*
- Studies of resonance in open-ocean e.g. Wunsch 1972, Platzman et al. 1981
- Studies of paleotides e.g. Egbert, Ray, Bills 2004, Arbic, MacAyeal, Mitrovica, Milne 2004, Arbic, Mitrovica, MacAyeal, Milne 2008, others

Shallow-water model (Arbic, Karsten, Garrett)



- Solve 1-D nonrotating linearized shallow water equations, driven by tidal potential $\eta_0 e^{i(kx + \omega t)}$, subject to no normal flow conditions at $x = -L_1, L_2$ and matching conditions for elevation and mass transport at $x = 0$
- Solutions illuminating and broad but more involved than solutions of ...

Coupled oscillator model (Arbic and Garrett)



Equilibrium positions

Governing equations—coupled oscillator model

$$\frac{d^2\zeta_1}{dt^2} + \delta_1\omega_1\frac{d\zeta_1}{dt} + \omega_1^2\zeta_1 = a\omega_1^2\cos(\omega t) + \epsilon\omega_2^2(\zeta_2 - \zeta_1)$$

$$\frac{d^2\zeta_2}{dt^2} + \delta_2\omega_2\frac{d\zeta_2}{dt} + \omega_2^2\zeta_2 = \omega_2^2\zeta_1$$

$$\omega_1^2 = \frac{k_1}{m_1}$$

$$\omega_2^2 = \frac{k_2}{m_2}$$

$$\epsilon = \frac{m_2}{m_1}$$

Solutions-coupled oscillator model

$$\zeta_j = \text{Re}[Z_j \exp(-i\omega t)], \quad j = 1, 2$$

$$Z_1 = \frac{a}{p - iq}, \quad Z_2 = A e^{i\theta} Z_1$$

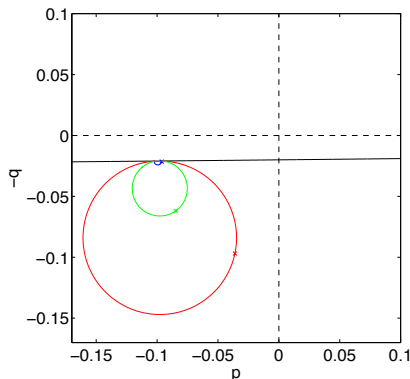
$$p = p_1 + \epsilon r^2 \left(1 - \frac{p_2}{p_2^2 + q_2^2}\right), \quad q = q_1 + \epsilon r^2 \left(\frac{q_2}{p_2^2 + q_2^2}\right)$$

$$p_j = 1 - r_j^2, \quad q_j = \delta_j r_j$$

$$A e^{i\theta} = \frac{1}{1 - r_2^2 - i\delta_2 r_2}$$

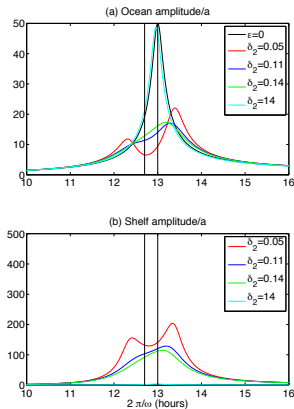
$$r_1 = \omega/\omega_1, \quad r_2 = \omega/\omega_2, \quad r = \omega_2/\omega_1$$

Coupled oscillator model: p and $-q$ vs r_2



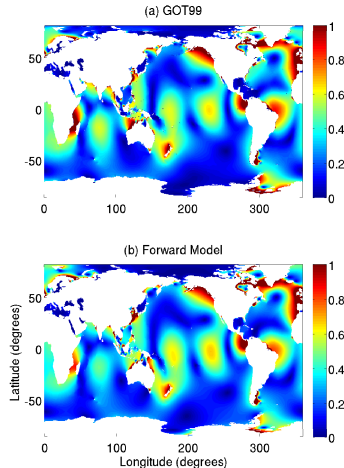
- Black curve: ocean by itself (no shelf), with $\delta_1=0.02$ and varying r_1
- Red/green/blue curves: $\delta_2=0.05/0.14/14$, with ϵr^2 fixed at 0.0063, $\delta_1=0.02$, $r_1=1.05$
- “x’s”: $r_2=1.02$

Coupled oscillator model: Ocean and shelf amplitudes vs frequency



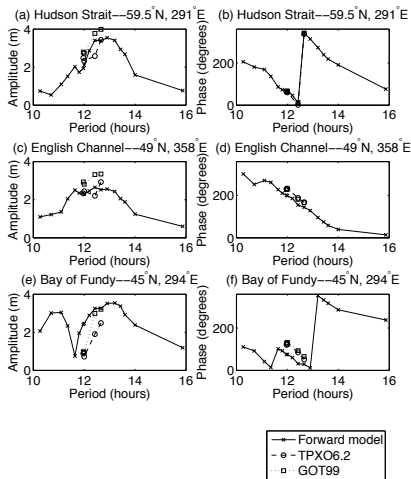
- Resonant periods of ocean and shelf are 13 and 12.7 hours, shown as vertical lines
- $\delta_1=0.02$, $\epsilon=0.006$

M_2 amplitude (m): Forward numerical model vs GOT99 satellite-constrained model

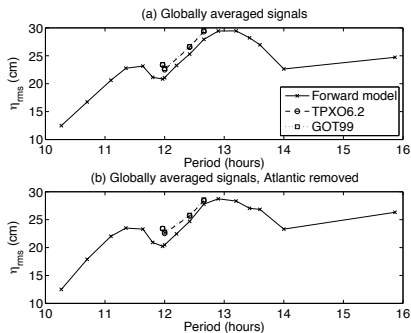


- Forward model: Arbic, Garner, Hallberg, Simmons 2004

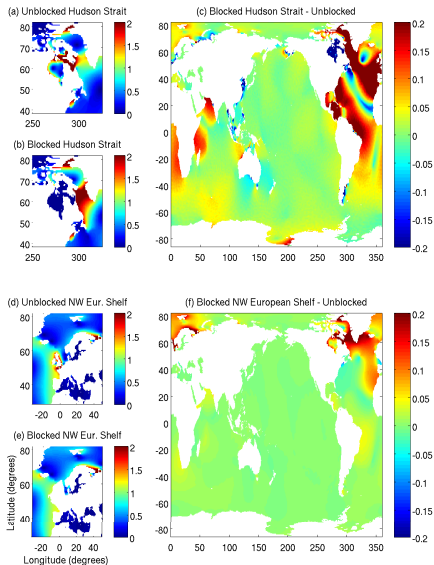
Coastal amplitudes and phases in frequency sweep of forward numerical model



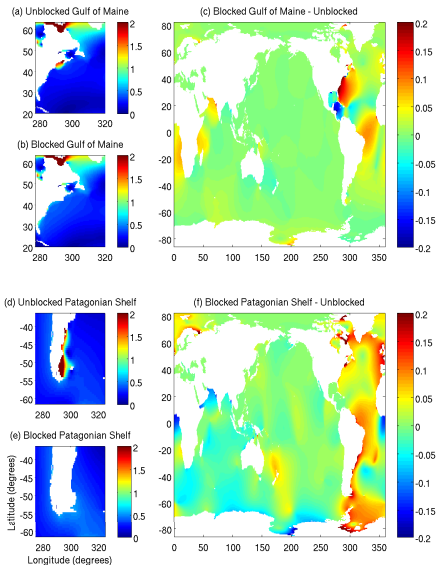
Open-ocean amplitudes in frequency sweep of forward numerical model



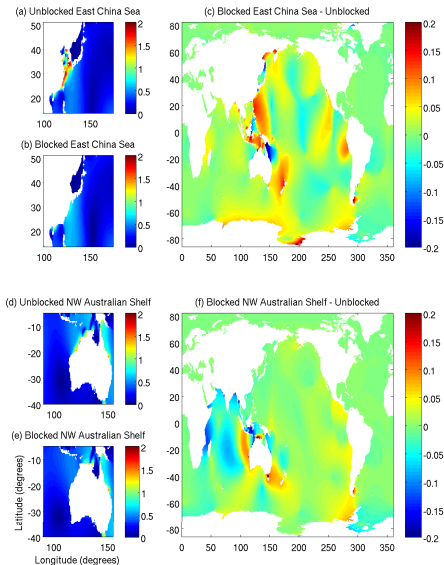
Back-effect of shelves on M_2 amplitudes (m)



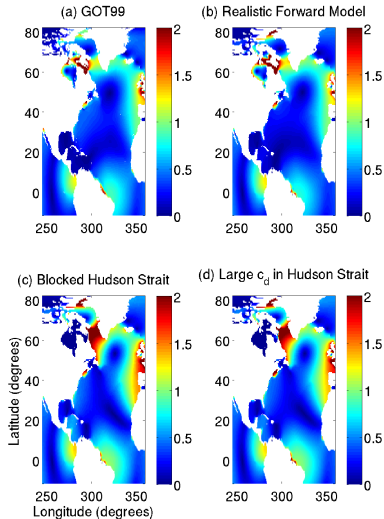
Back-effect of shelves on M_2 amplitudes (m)



Back-effect of shelves on M_2 amplitudes (m)



Numerical model: Effect of shelf friction on M_2 amplitudes (m)



Summary–Part II (Resonance of barotropic tides)

- Two analytical models—a linearized shallow water model and a coupled oscillator model—both predict that 1) tides will resonate as the frequency of the astronomical forcing changes, and coupling of shelf and open-ocean will result in a “double bump” in frequency sweep plots, 2) resonant shelves will tend to reduce resonant open-ocean tides, 3) effect of a shelf with very large friction will be similar to effect of blocking out shelf completely.
- Numerical experiments largely confirm predictions of analytical models—frequency sweeps show a resonance with double bumps, and both removal of resonant shelves from the model domain, and a strong increase in shelf friction, tend to increase open-ocean tides.
- “Back-effect” of shelves upon open-ocean tides is relevant to understanding ice-age tides, which took place with much lower sea level and hence a much reduced shelf area.
- Follow-on studies include tidal response to changing sea levels and stratification of present-day and potential future.

Motivation–Part III (Concurrent simulation of tides and an eddying general circulation)

- Ocean mixing driven partly by breaking internal gravity waves, which source partly from tides. First global models of internal tides, run with Hallberg Isopycnal Model (Arbic et al. 2004, Simmons et al. 2004; hereafter AGHS and SHA), included only tidal forcing and were run with horizontally uniform stratification.
- Desirable to have model in which generation and propagation of internal tides takes place in more realistic, horizontally varying stratification, and potential exists for interactions between tidal and non-tidal flows.
- Have recently completed 5-year global simulation of HYbrid Coordinate Ocean Model (HYCOM) with 32 layers in the vertical direction, $1/12.5^\circ$ horizontal resolution, and forcing of eight largest tidal constituents in addition to wind- and buoyancy-forcing.

Need for parameterized wave drag in baroclinic tide models

- 2/3 of tidal energy dissipation takes place in shallow seas (mainly via quadratic BBL drag), and 1/3 takes place in abyss, via internal tide breaking over topography (Egbert and Ray 2000).
- Several recent studies: inserting parameterized topographic wave drag greatly improves SSH accuracy of forward barotropic tide models. AGHS: accuracy affected by wave drag because globally integrated energies of model are affected.
- What should one do in baroclinic forward tide models, in which low mode internal tides are resolved?
- Main two-layer simulations of AGHS include parameterized topographic wave drag
 $r(lat, lon)u_{bottom}$ in bottom layer, representing unresolved generation and breaking of high modes near bottom. Main baroclinic simulations of SHA do not include parameterized wave drag.

Barotropic energies and surface elevation errors wrt altimetry in AGHS and SHA

- ER2003–Egbert and Ray (2003) – satellite-constrained models
- Energy in units of $10^{17} J$
- Numbers in parantheses denote percentage of sea surface elevation variance captured

Model	APE	KE	Error (cm)
ER2003	1.34	1.78	–
AGHS main	1.48	1.73	7.37 (92.4)
AGHS no drag	3.18	3.46	17.14 (58.8)
SHA main	4.37	5.09	23.35 (23.5)
SHA appendix	1.66	2.03	9.88 (86.3)

- SHA main: ~ 1 TW of energy is converted from barotropic to baroclinic modes, but waves do not break and total BC+BT energy is not removed from model, leaving BT energies too high.

New complication for topographic drag in HYCOM simulation

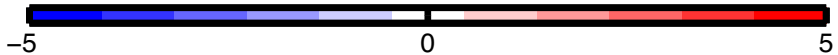
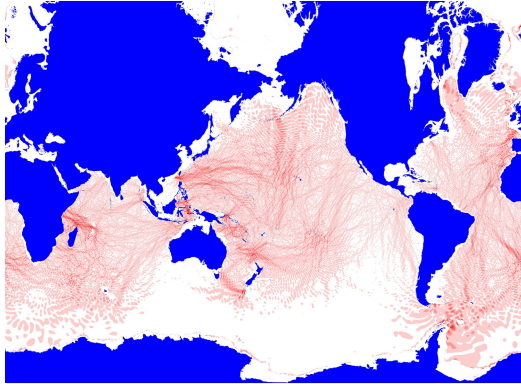
- Topographic wave drag probably acts on low-frequency motions (Nikurashin 2008) as well as tides.
- But the action is different for the two types of motions (Bell 1975).
- Therefore, a separation of the model bottom flows into tidal versus non-tidal components is desirable.
- This separation is done crudely with a 25-hour running average of the bottom flow.
- Plots being made as we speak to show effect of topographic wave drag on non-tidal bottom flows.

Elevation errors in HYCOM run

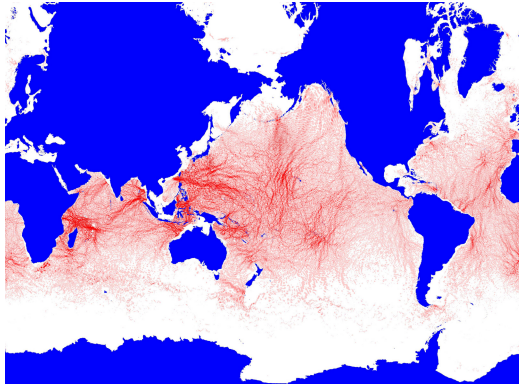
- Computed wrt standard set of 102 pelagic tide gauges (Shum et al. 1997)

Constituent	Signal (cm)	Error (cm)
Q ₁	1.62	0.68 (82.1)
O ₁	7.76	2.48 (89.7)
P ₁	3.62	0.79 (95.2)
K ₁	11.26	2.48 (95.1)
N ₂	6.86	1.40 (95.9)
M ₂	33.22	8.26 (93.8)
S ₂	12.62	5.17 (83.2)
K ₂	3.43	1.65 (76.9)
RSS	39.04	10.63 (92.6)

Amplitude of M_2 internal tide signature in steric ssh: Two-layer tide-only run

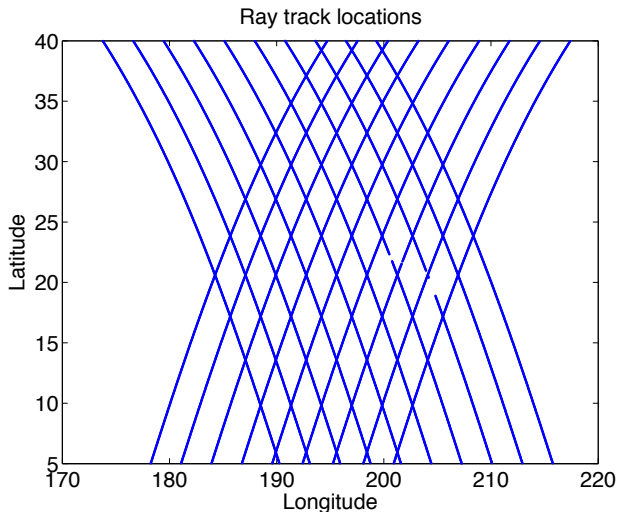


Amplitude of M_2 internal tide signature in steric ssh: Warm-up wind-plus-tides run

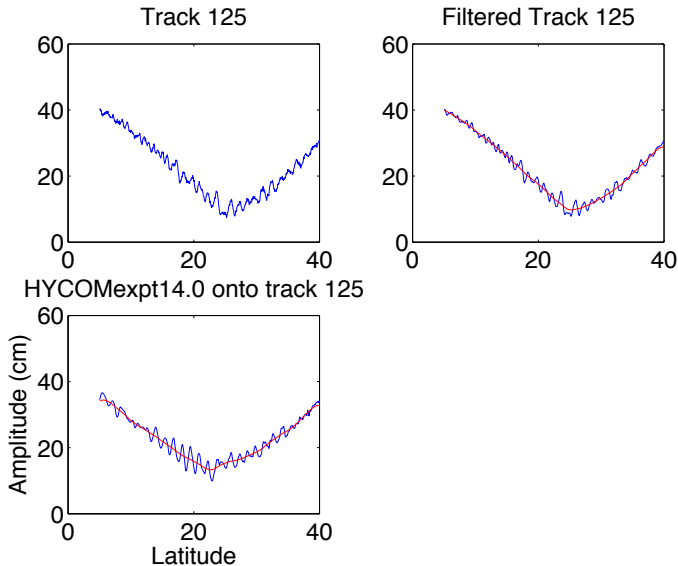


Altimeter tracks around Hawai'i

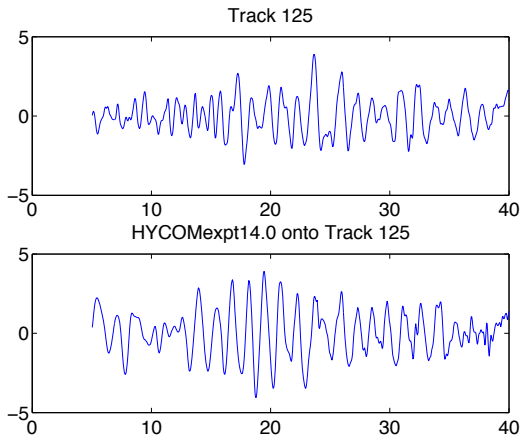
- Data obtained by personal communication with Richard Ray.



M_2 amplitudes along track 125



M_2 internal tide perturbations to SSH

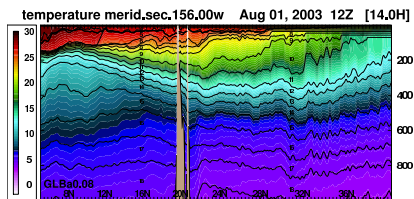
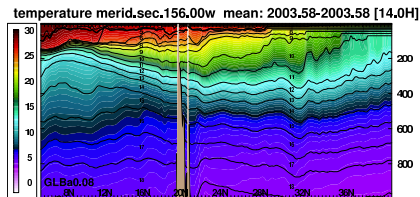
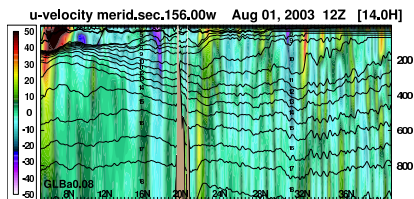
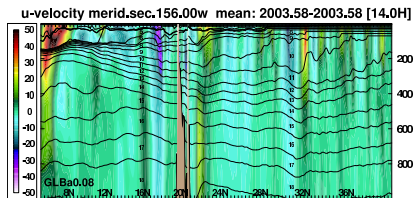


- RMS amplitudes of perturbations along all tracks: 0.59 cm (altimeter data), 0.73 cm (HYCOM), 0.76 cm (SHA), 0.28 cm (AGHS)

Vertical section of model through Hawai'i

25-hour mean

Snapshot



Summary–Part III (Concurrent simulation of tides and an eddying general circulation)

- Concurrent simulation of tides and eddying general circulation achieved in global HYCOM.
- Model captures 93% of open-ocean SSH variance of eight largest tidal constituents.
- Magnitude of internal tide perturbations to SSH around Hawai'i similar to that in altimeter data \Rightarrow HYCOM has reasonably accurate BT and BC tides, unlike main BC solutions in SHA (BT tide too energetic) and AGHS (BC tide too weak).
- In contrast to earlier global baroclinic tide runs, HYCOM run has horizontally varying stratification.
- 25-hour running average utilized to separate tidal from non-tidal motions in topographic wave drag scheme.
- HYCOM run likely to be useful for feasibility studies of planned wide-swath satellite altimeter, for which internal tides are expected to be a large source of noise.